Since January 2020 Elsevier has created a COVID-19 resource centre with free information in English and Mandarin on the novel coronavirus COVID-19. The COVID-19 resource centre is hosted on Elsevier Connect, the company's public news and information website.

Journal of Molecular Graphics and Modelling 111 (2022) 108113

Contents lists available at ScienceDirect

Journal of Molecular Graphics and Modelling

journal homepage: www.elsevier.com/locate/jmgm

Identification of potent food constituents as SARS-CoV-2 papain-like protease modulators through advanced pharmacoinformatics approaches

Shovonlal Bhowmick [a], Achintya Saha [a,**], Nora Abdullah AlFaris [b], Jozaa Zaidan ALTamimi [b], Zeid A. ALOthman [c], Tahany Saleh Aldayel [b], Saikh Mohammad Wabaidur [c], Md Ataul Islam [d,*]

[a] Department of Chemical Technology, University of Calcutta, 92, A.P.C. Road, Kolkata, 700009, India
[b] Nutrition and Food Science, Department of Physical Sport Science, Princess Nourah bint Abdulrahman University, P. O. Box 84428, Riyadh, 11671, Saudi Arabia
[c] Department of Chemistry, P.O. Box 2455, College of Science, King Saud University, Riyadh, 11451, Saudi Arabia
[d] Division of Pharmacy and Optometry, School of Health Sciences, Faculty of Biology, Medicine and Health, University of Manchester, Oxford Road, Manchester, M13 9PL, United Kingdom

ARTICLE INFO

Keywords:
SARS-CoV-2 PLpro
Food compounds
Virtual screening
Molecular docking
Molecular dynamics
MM-GBSA

ABSTRACT

The current ongoing pandemic of COVID-19 urges immediate treatment measures for controlling the highly contagious SARS-CoV-2 infections. The papain-like protease (PLpro), which is released from nsp3, is presently being evaluated as a significant anti-viral drug target for COVID-19 therapy development. Particularly, PLpro is implicated in the cleavage of viral polyproteins and antagonizes the host innate immune response through its deubiquitinating and deISGylating actions, thus making it a high-profile antiviral therapeutic target. The present study reports a few specific food compounds that can bind tightly with the SARS-CoV-2 PLpro protein identified through extensive computational screening techniques. Precisely, extensive advanced computational approaches combining target-based virtual screening, particularly employing sub-structure based similarity search, molecular docking, molecular dynamics (MD) simulations, and MM-GBSA based binding free energy calculations have been employed for the identification of the most promising food compounds with substantial functional implications as SARS-CoV-2 PLpro protein inhibitors/modulators. Observations from the present research investigation also provide a deeper understanding of the binding modes of the proposed four food compounds with SARS-CoV-2 PLpro protein. In docking analyses, all compounds have established essential inter-molecular interaction profiles at the active site cavity of the SARS-CoV-2 PLpro protein. Similarly, the long-range 100 ns conventional MD simulation studies also provided an in-depth understanding of probable interactions and dynamic behaviour of the SARS-CoV-2 PLpro protein-food compound complexes. Binding free energies of all molecular systems revealed a strong interaction affinity of food compounds towards the SARS-CoV-2 PLpro protein. Moreover, clear-cut comparative analyses against the known standard inhibitor also suggest that proposed food compounds may act as potential active chemical entities for modulating the action of the SARS-CoV-2 PLpro protein.

1. Introduction

Among many attractive antiviral drug targets of severe acute respiratory syndrome coronavirus 2 (SARS-CoV-2), the papain-like cysteine protease (PLpro) which is encoded within nsp3 represents to be a very promising and important drug target for the development of anti–COVID-19 drug therapeutics [1–5]. Due to similarity in the structural organization with other protease families including SARS-CoV-1 [6], targeting the SARS-CoV-2 PLpro can surely dictate some potential therapeutic value for the life-threatening COVID-19 pandemic management. A detailed understanding of the molecular function of SARS-CoV-2 PLpro demonstrated its involvement in virus replication mechanism through the processing of viral polyproteins and also in cleaving proteinaceous post-translational modifications on host proteins [6,7]. However, the ongoing pandemic of COVID-19 urges a much better understanding of viral pathogenesis mechanisms for efficiently developing safe and target selective drug therapeutic interventions. Importantly, the SARS-CoV-2 viral polyproteins are mostly processed by the

* Corresponding author.
** Corresponding author.
E-mail addresses: achintya_saha@yahoo.com (A. Saha), ataul.islam80@gmail.com (M.A. Islam).

https://doi.org/10.1016/j.jmgm.2021.108113
Received 16 August 2021; Received in revised form 5 December 2021; Accepted 18 December 2021
Available online 21 December 2021

enzymes 3-chymotrypsin like protease (3CLpro) and PLpro. Due to the multifunctional biological activities as well as an important role in governing pathogenesis, targeting SARS-CoV-2 viral proteases or any proteolytic enzymes, either main protease (3CLpro or Mpro, encoded by nsp5) or PLpro protein has demonstrated an added advantage for therapeutic development to treat COVID-19 [6,8,9]. Economic and health crisises have been extensively observed and encountered at the global level due to COVID-19 emergence in a much devastating way than the previous coronavirus outbreaks reported in 2002 and 2012, in China and in Saudi Arabia, respectively [10]. According to the World Health Organization's (WHO) "Weekly Operational Update on COVID-19″ published on November 30, 2021, there were 260,493,573 confirmed SARS-CoV-2 infected patients and 5,195,354 deaths globally. The severity of this deadly infection is still active in some parts of the globe, including India, Brazil, and the United States of America, due to occurrence of 2nd or 3rd waves, however no active chemotherapeutic agents have been developed yet to tackle this pandemic.

The tetrapeptide LXGG pattern present between viral proteins nsp1 and nsp2, nsp2 and nsp3, and nsp3 and nsp4 (nsp1/2, nsp2/3, and nsp3/4) is recognized by this PLpro enzyme. The release of nsp1, nsp2, and nsp3 proteins, which are required for viral replication, is caused by the hydrolysis of the peptide bond on the carboxyl side of glycine at the P1 position [11]. Earlier, *in vitro* studies have revealed that SARS-CoV PLpro has two additional proteolytic activities: ubiquitin (Ub) and Ub-like (Ubl) protein ISG15 (interferon-induced gene 15) removal from cellular proteins [3,7]. SARS-CoV PLpro hydrolyzes ubiquitinated and ISGylated substrates more efficiently than small substrates bearing the C-terminal LRGG motif. Such an important discovery pointed to a more sophisticated method of substrate identification than only the contact of the enzyme's S4–S1 pockets with the tetrapeptide fragment [12,13]. In general, SARS-CoV PLpro has two unique Ub binding subsites (SUb1 and SUb2) that identify Lys48-linked polyUb chains for polyUb chain editing and/or deubiquitination of polyubiquitinated proteins [13]. The structural and functional organization of SARS-CoV PLpro demonstrated that the active site of PLpro is made up of a catalytic trio of Cys111–His272–Asp286 residues [5]. Earlier, different CoVs PLpro were investigated widely, and found to be located at the intersection of the thumb and palm sub-domains [14,15]. Particularly, PLpro's proteolytic actions are carried out through a catalytic cysteine-protease cycle in which Cys111 operates as a nucleophile, His272 as a general acid/base, and Asp286 is connected to the histidine to help it align and deprotonate Cys111 [16]. For the development of selective SARS-CoV-2 candidate drug compounds, targeting the catalytic pocket is desirable since it could allosterically inhibit the active site by causing loop closure. Antiviral small molecules identified based on the PLpro structure guided approach may have a benefit in not only inhibiting CoVs replication but also in limiting the dysregulation of signaling cascades in CoVs infected cells, resulting in the death of uninfected neighboring cells. Hence, PLpro is an important target for *anti*-COVID drug development.

Several scientific communities or groups have employed different computational techniques to identify small molecule inhibitors of the SARS-CoV-2 PLpro protein [8,17–25], however identification of active food constituents-based modulators or inhibitors have yet to be deployed in a larger spectrum. Over the past decades, research studies conducted on bioactive food chemicals have been demonstrated to possess both, either deleterious or beneficial function in human health and many diseases including type 2 diabetes, neurological disorder, cancer, obesity, and cardiovascular problems, based on several physiopathological and clinical research [26–30]. According to scientific research and epidemiological data, intake of bioactive natural food products, such as fruits and vegetables, is linked to increased potential health advantages, including a lower risk of numerous chronic diseases [29,31,32]. Some commonly known bioactive compounds found in various sources of food products, *viz.* quercetin, ascorbic acid, curcumin, gallic acid, polyphenols, catechins, anthocyanins, oleuropein, resveratrol, epigallocatechin, capsaicin, caffeine, sulforaphane, ellagic acid, and other food containing biomolecules, may directly contribute to the prevention, treatment, or management of better health conditions [28,29,33,34]. Understanding the molecular impacts of various bioactive food components in the advancement of such disease-modifying implications, however, has remained a mystery. Specifically, a large number of clinical experiments in diverse human cell and tissue samples have shown that bioactive dietary components have a significant role in selective gene expression by influencing phosphorylation and post-translational events as well as large scale epigenetic alteration modulation or many other proteomic modifications [33,35–38]. Furthermore, there is evidence to explore the anti-viral and immune system modulating properties of various traditional or specific food constituents, including prevention of coronavirus infection and application in cancer [39–44]. Therefore, in the present study, an exhaustive computational approach including sub-structure based similarity search against available non-covalent inhibitor, molecular docking and dynamics simulations, and MM-GBSA based binding free energy estimation of protein-ligand complexes has been employed. According to the present study findings, four food compounds, *viz.* FDB001395, FDB029219, FDB030757, and FDB031079, have been found with a significant binding affinity towards SARS-CoV-2 PLpro, and hence can be implicated as strong modulators for PLpro protein.

2. Materials and methods

2.1. Selection and preparation of food compounds and SARS-CoV-2 PLpro protein

Approximately a total of 70477 food chemicals were collected from FooDB (available at www.fooddb.ca). All those FooDB database chemicals were downloaded in SMILE format and then converted into two-dimensional (2D) molecular structural data format (.sdf) files. Following that, in Discovery Studio, all 2D representations of transformed molecules were prepared to remove redundancies, bad valency, and then transformed to a three-dimensional (3D) molecular format. With the help of Open Babel, an open-source software tool for molecular file format compatibility, the entire provided dataset was converted to pdbqt. The '.pdbqt' is the mandatory format required in AutoDock Vina (ADV) tool [45]. Such a format is quite similar to the Protein Data Bank (PDB) representation but it includes partial charges and AutoDock 4 atom types. Additionally, the attached non-covalent inhibitor was prepared using the same protocol and considered as a control compound in the current study for the assessment of outcomes.

On the other hand, the SARS-CoV-2 PLpro crystal structure was obtained from the PDB repository (PDB ID: 7JIW) [14]. In order to prepare the protein structure, an appropriate number of polar hydrogen atoms and Gasteiger charges were added/adjusted to the SARS-CoV-2 PLpro crystal structure using AutoDock tool (ADT). The crystal structure was stripped of water (H_2O) molecules and other tiny molecules linked to them. Finally, the atoms were assigned the AD4 type and saved as.pdbqt file. It has been reported that the catalytic trio of Cys111–His272–Asp286 amino acid residues are required to render pathogenicity inactive, decreased, and/or conceded. Therefore, the grid box for molecular docking was chosen around the catalytic triads as mentioned above. Along the X-, Y-, and Z-axes, the binding site's center coordinates are 51.69, 31.29, and −2.96 Å, respectively. The grid's dimensions were set to 40 X 40 × 40 Å along with the X-, Y-, and Z-axes, respectively. The grid spacing was defined as 0.375 Å.

2.2. Substructure search against known standard non-covalent inhibitors using ICM-Molsoft

Fingerprint similarity (FPS) based substructure search was carried out using ICM-Molsoft (version 3.9-1b) [46]. In particular, in the ICM-Molsoft user interface, 'search type' was specified as 'FP similarity' search, and 'Max distance' was assigned as 0.8 against non-covalent

inhibitor VBY as the query molecule for generation of most similar compounds as outcomes from the similarity search. The rest of the parameter was kept as default during search execution. In particular, using this FP similarity search method, any fingerprint inside a structure may be searched against any given database (here the curated FooDB database was used). The searched out compounds were saved in .sdf format for use in further applications.

2.3. Molecular docking using AutoDock Vina

The molecular docking execution was carried out for all ligands using the ADV standard protocol [45,47]. Particularly, the information for the prepared SARS-CoV-2 PLpro protein (as a receptor), ligands, and grid file was saved in text format in the configuration file and further used in the widely accepted docking application program. The docking was carried out using the ADV application, which was installed on a Linux-based operating system. The binding affinity score was used as a screening criterion once the molecular docking was completed successfully. As a result, a user defined binding affinity threshold score value of −7.00 kcal/mol was used for further screening criteria. More details of the employed ADV protocol can be found in our previous studies [48,49].

2.4. Binding affinity prediction by K_{Deep} – a neural network method

The obtained screened molecules from the ADV tool were further subjected to relative binding affinity prediction by the K_{Deep} tool [50] that followed a neural network method. Particularly, the K_{DEEP} web-based application is a cutting-edge 3D convolutional neural network-based protein-ligand binding affinity prediction tool [50] that was used in this investigation to determine the binding affinity of each dietary food compound with SARS-CoV-2 PLpro protein. The K_{DEEP} tool works based on the deep convolutional neural networks (DCNNs) model, which has already been pre-trained, tested, and verified with the PDBbind v.2016 database. Precisely, during execution, the K_{DEEP} initially divides the binding site into 8 different pharmacophoric-like features/descriptors (such as hydrogen-bond donor or acceptor, aromatic, hydrophobic, metallic, positive, or negative ionizable, and total excluded volume) before using those descriptors for model generation and binding affinity prediction. The above mentioned web-application based programme is publicly accessible at https://www.playmolecule.com/Kdeep/. To run the K_{DEEP} tool, all compounds were selected from ADV, having −7.00 kcal/mol score given as input, and other features were left as default.

2.5. Molecular dynamic simulations

To understand the dynamic behaviour of the investigated SARS-CoV-2 PLpro protein and selected four food compounds under a time-dependent microcanonical ensemble, long range MD simulations were performed. Particularly, an all-atoms conventional MD simulation over a time duration of 100 ns was used to thoroughly reconnoitre the structural behaviour of dietary compounds attached to SARS-CoV-2 PLpro protein in dynamic states. The Amber20 software package loaded on a Linux operating system environment with a system configuration of 10th Generation Intel Core i9-10885H and NVIDIA® GeForce RTXTM 2070 was used to run the entire MD simulation. Each SARS-CoV-2 PLpro protein and food compound-complex was submerged in the TIP3P water model's truncated octahedron [51]. In addition, a suitable or required amount of Na^+ and Cl^- were added to the entire system in order to neutralise the complex system, and the system's ionic strength was set to 0.1 M to maintain the physiological pH during simulation. The topology files for protein and small molecules were generated using the ff14SB and GAFF2 force fields, respectively [52,53]. Amber20's pmemd.cuda module was used to run the simulation execution [54]. The entire protein-lignad system's temperature was maintained at 300K using a Langevin thermostat. The collision frequency was tuned to 2 ps^{-1} at 1 atm using the Monte Carlo barostat. The SHAKE algorithm was used to limit the covalent bonds linked with hydrogen atoms. The short-range electrostatic interactions were addressed using an 8 Å threshold, whereas the long-range electrostatic interactions were addressed using the particle mesh Ewald technique. The solvent and ions were equilibrated over a 10 ns time period prior to the commencement of simulation production using NVT and NPT ensembles. After completion of the MD simulation run, to investigate the stability of all protein-ligand complexes, a number of trajectory analyzing parameters were estimated from the entire simulation trajectories, including RMSD, root-mean-square fluctuation (RMSF), radius of gyration (RoG), solvent accessible surface area (SASA), and a complete hydrogen bond interaction profiles.

2.6. Binding free energy calculation through MM-GBSA approach

The interaction affinity of any small molecule for a stable macromolecular complex formation can be explained by its binding free energy. Therefore, binding free energy derived using MD simulation trajectories is said to be more precise and reliable than binding energy derived through molecular docking. In the present study, the binding free energy was calculated using the molecular mechanics-generalized born surface area (MM-GBSA) method [55] using the last 10000 frames of each system. The same approach was used in our previous published work [56]. In particular, the following mathematical derivation was followed for MM-GBSA based binding free energy estimation for the protein-ligand complexes. The ensemble of MD simulation trajectories of PLpro bound with finally proposed dietary compounds were used to calculate the ΔG_{bind} value for each complex. The following stepwise expressions were used for the ΔG_{bind} calculation.

$$\Delta G_{bind} = G_{com} - (G_{rec} + G_{lig}) \quad (1)$$

$$\Delta G_{bind} = \Delta H - T\Delta S \quad (2)$$

$$\Delta G_{bind} = \Delta E_{MM} + \Delta G_{sol} - T\Delta S \quad (3)$$

$$\Delta E_{MM} = \Delta E_{int} + \Delta E_{ele} + \Delta E_{vdw} \quad (4)$$

$$\Delta G_{sol} = \Delta G_{pol} + \Delta G_{npol} \quad (5)$$

where, the ΔG_{bind} is achieved (equation (1)) through subtraction of added free energy of the receptor (ΔG_{rec}) and ligand (ΔG_{lig}) from the free energy of complex (ΔG_{com}). From the expression (2) it can be seen that the ΔG_{bind} is the difference between two terms, enthalpy (ΔH) and entropy (TΔS). The GBSA was used to get the enthalpy term, whereas, entropy was achieved from the normal mode analysis (NAM) and interaction entropy (IE) methods. It is important to note that the ΔH is signified by molecular mechanical energy (ΔE_{MM}) and solvation free energy (ΔE_{sol}). The ΔE_{MM} is the combination of intra-molecular (ΔE_{int}), electrostatic (ΔE_{ele}) and the van der Waals interaction (ΔE_{vdw}) energies. Further, the free energy of solvation (ΔG_{sol}) can be represented by the addition of polar (ΔG_{pol}) and non-polar (ΔG_{npol}) energies. Finally, it worth to indicate that the modified Generalized Born (GB) [57] was applied to get the ΔG_{pol} and ΔG_{npol} those were achieved from the LCPO algorithm [58] which is based on SASA.

3. Results and discussion

3.1. Virtual screening and sub-structure based similarity searching

Structure-based virtual screening is a very promising computational drug discovery technique for finding out potential lead-like chemicals from any chemical database for a certain bio-macromolecular protein target. Because chemical databases contain a large number of chemical entities, they can be quickly analyzed for possible interactions

employing various advanced computational methods or algorithms. In the same context, a set of more than seventy thousand food constituents was retrieved from FooDB and was further manually curated the entire database and then screened against SARS-CoV-2 PLpro protein using several comprehensive computational methodologies. Initially, in the present study, a sub-structure based similarity search followed by molecular docking and conventional dynamics simulations based methodologies were utilized to find some prospective food chemical entities which may make stable interactions/contacts with SARS-CoV-2 PLpro protein at the active site residues and so can modulate or suppress its biological activity. The illustration of the entire workflow is given in Fig. 1.

Particularly, the entire FooDB database (containing ~ 70477 compounds) was initially curated using a number of criteria like removal of

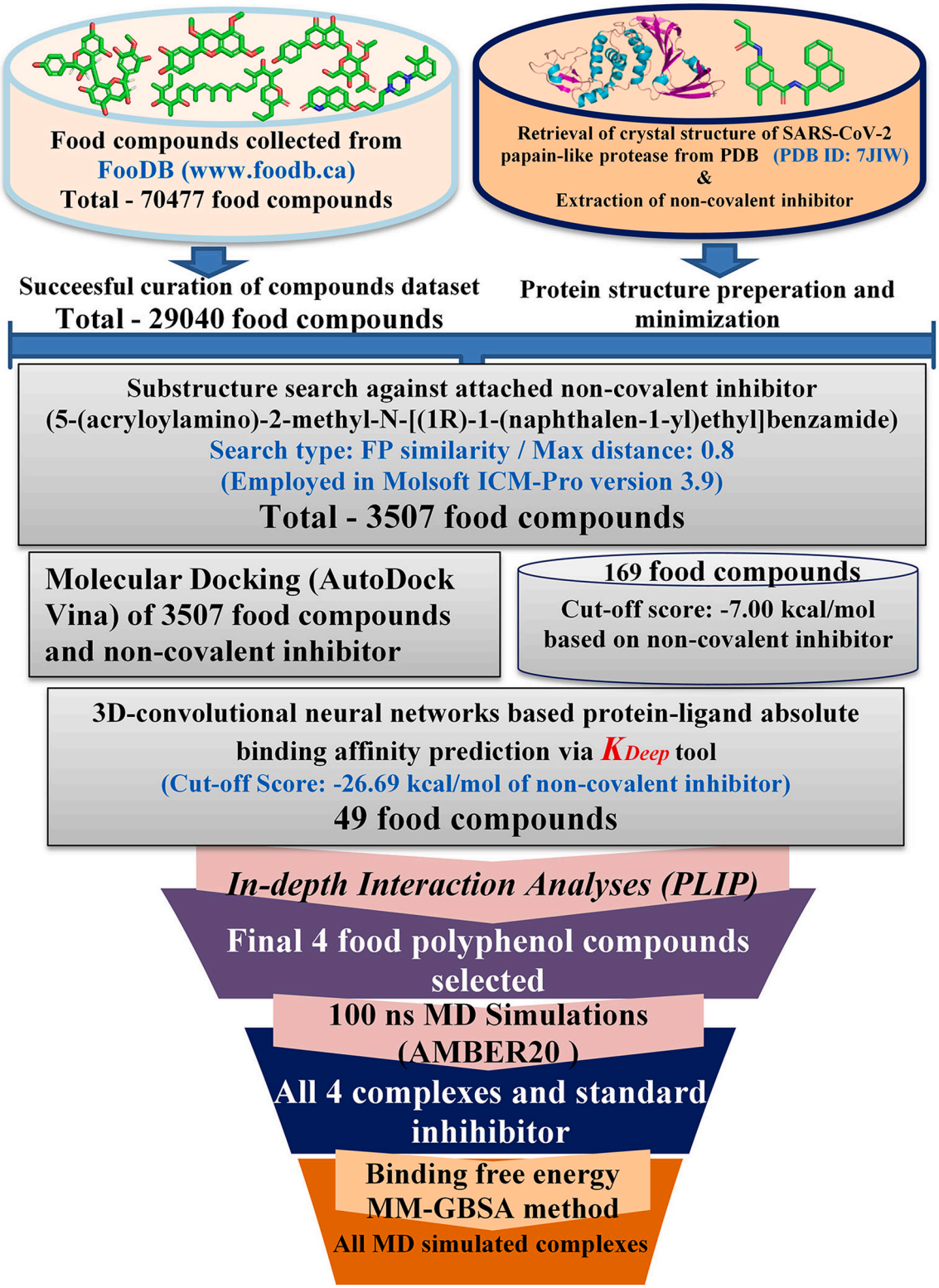

Fig. 1. Virtual screening and sub-structure based similarity search workflow for identification of PLpro inhibitors/modulators.

too small molecules or molecules containing only atoms, valence error compounds, presence of salt ions, etc., and after data curation, ~29040 molecules were found to be suitable for further screening. The non-covalent co-crystal inhibitor [5-(acryloylamino)-2-methyl-N-[(1R)-1-(naphthalen-1-yl)ethyl]benzamide] attached with selected SARS-CoV-2 PLpro protein was used as the template for sub-structure based similarity search against the above curated set of molecules. The above-mentioned non-covalent co-crystal inhibitor is also known as VBY and in the current study, it will refer to the same, hereafter.

A stringent fingerprint based sub-structure search was performed to dig out food chemical entities which probably have similar structural or chemical properties to the non-covalent inhibitor like VBY. Precisely, the molecular fingerprint based search was performed in Molsoft ICM-Pro and the maximum distance for similarity search was given as 0.8. The fingerprint based similarity search enables any fingerprint within a structure to be searched for the given database. Herein, the employed similarity serach method calculated the Tanimoto coefficient [59] index (specified as 0.8) using chemical fingerprints. The non-covalent inhibitor VBY was searched against the curated FooDB database. Importantly, reason behind employing such fingerprint based similarity search was the similar property principle approach which states that molecules with similar structural similarities probably tend to show similar characteristics [60]. In terms of drug development concept, fingerprints implies structural motifs, fragments, or functional groups which can be used as some suitable descriptors for predictive modeling. Based on such significant similarity index, 3507 molecules were screened out from the similarity search analysis in Molsoft ICM-Pro. For further assessment, the above remaining molecules along with VBY were subjected to molecular docking study in the ADV. On successful docking execution of all compounds, the binding energy of each molecule was explored. The binding energy of the standard compound VBY was found to be −7.00 kcal/mol and it was considered as a threshold score to further reduce the chemical space of the docked molecules. On the otherhand, the binding energy of the docked dietary 3507 compounds was found to be within the range of −3.20 to −11.90 kcal/mol. While applying the threshold binding energy score (−7.00 kcal/mol) for sequential filtration of most superior dietary compounds, a total of 169 food compounds were retained. Further, the K_{Deep} module was used to calculate the protein-ligand absolute binding energy of the remaining compounds in the above step along with VBY. Similar to the above user defined cut-off score, the binding free of VBY was used as a threshold (−26.69 kcal/-mol) and found 49 food compounds to possess better binding affinity in comparison to VBY. The binding pose, orientation and binding interaction pattern of each of the above molecules were explored and compared with VBY. Particularly, absolute binding energy score, association of total number of intermolecular interactions with different amino acid residues of PLpro protein, and site of interactions were critically checked and compared against the standard compound VBY, for selection of potential dietary compounds as selecitive modulators/inhibitors for SARS-CoV-2 PLpro protein. Finally, based on the above parameters, four molecules were found to be promising for modulation or inhibition of SARS-CoV-2 PLpro activity. Further, interactions stability and binding affinity potential of each molecule towards PLpro were explored through 100 ns MD simulation study. Two-dimensional (2D) representation of the final four molecules is given in Fig. 2. Precisely, the identified proposed compounds FDB001395, FDB029219, FDB030757, and FDB031079 are commonly known as Diosbulbinoside D, Estrone-2,3-quinone, cyanidin 5-O-β-D-glucoside, and *p*-coumaroyltriacetic acid lactone. FDB001395 (Diosbulbinoside D) belong to the class of organic compounds known as cholines and found in different food products such as fenugreeks, calabash, barley, cauliflowers and eggs etc. Compounds FDB029219 and FDB030757 (Estrone-2,3-quinone and cyanidin 5-O-β-D-glucoside) belong to the classes of compounds such as catechol estrogens and flavonoid o-glycosides, respectively. Another compound FDB031079 (*p*-coumaroyltriacetic acid lactone) belongs to the class of compound hydroxycinnamic acid and their derivatives. They usually found in foods like yellow zucchini, lowbush blueberry, fruits, and napa cabbage etc.

3.2. *Molecular docking and K_{Deep} based binding interaction analyses of food compounds*

The binding interactions analysis of the final proposed four food compounds (Fig. 2) were critically explored using the protein-ligand interaction profiler (PLIP) web tool [61]. Both the binding interaction profile and the binding mode of all four molecules are given in Fig. 3. Molecular docking based binding affinity scores of finally selected proposed food compounds FDB001395, FDB029219, FDB030757,

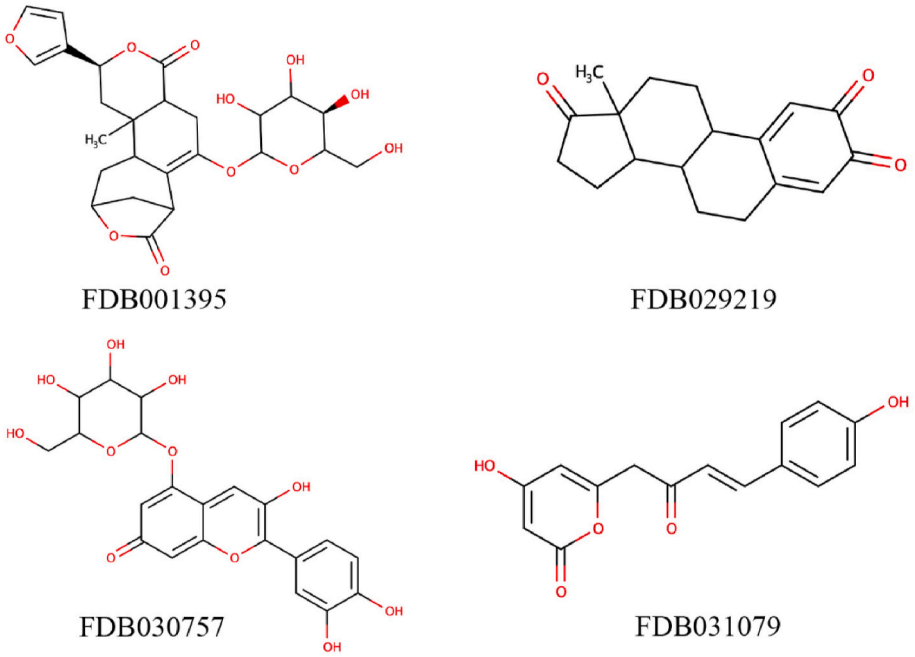

Fig. 2. Two-dimensional (2D) structural representation of final SARS-CoV-2 PLpro inhibitors/modulators.

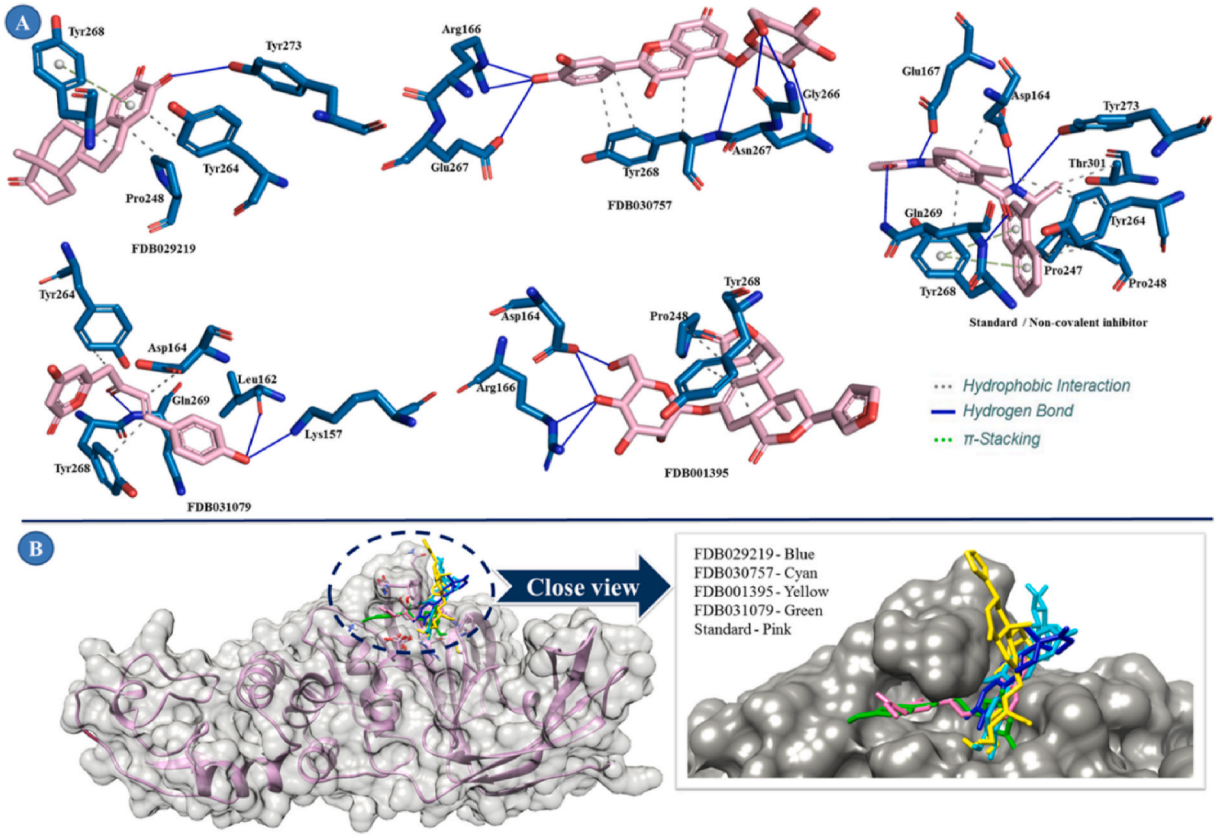

Fig. 3. A) Molecular binding interactions of proposed food compounds bound with SARS-CoV-2 PLpro protein obtained in docking analyses, B) Binding mode of proposed food compounds (displayed in stick) inside the active site cavity of SARS-CoV-2 PLpro protein (displayed in surface view presentation).

FDB031079, and standard inhibitor VBY were found to be −7.30, −7.30, −7.00, −7.40 and −7.00 kcal/mol, respectively. Whereas the K_{Deep} based binding energy was estimated as −32.83, −33.63, −35.15, −34.57, and −26.69 kcal/mol for compounds FDB001395, FDB029219, FDB030757, FDB031079, and standard non-covalent inhibitor VBY, respectively. Binding interaction analyses revealed that all molecules were found to form a number of intermolecular interactions such as hydrogen bonds (HB), hydrophobic and pi(π)-stacking interactions, etc. Initially, to check the reproducibility of the employed docking protocol, the interactions and binding mode between the PLpro and co-crystallized non-covalent inhibitor VBY were explored by superimposing the originally attached ligand and re-docked VBY ligand poses and found their RMSD value of 1.61 Å. The superimposed re-dock pose of the standard ligand VBY and originally attached co-crystallized ligand VBY was derived from the re-docking protocol and depicted in Fig. S1 (Supplementary file). It was truly interesting to observe the study finding that re-docking protocol was successfully able to reporduce a nearly identical binding orientation for the ligand VBY at the active site of the PLpro protein, and hence indicating true efficiency of the utilized docking protocol. The binding interaction profile of VBY was revealed by the HB interactions with amino acid residues Asp164, Glu167, Gln269, and Tyr273 of SARS-CoV-2 PLpro. Moreover, few other residues such as Asp164, Pro247, Pro248, Tyr264, Tyr268, and Thr301 were seen to connect with VBY through hydrophobic bonds. Beyond that residue Tyr268 also formed two pi-stacking interactions with VBY. Similar to co-crystal ligand VBY, Asp164 formed two HB interactions with two different hydroxyl groups attached to the pyran ring in FDB001395. One of the above hydroxyl groups was found to be crucial in forming two HB interactions with Arg166. Cyclohexene ring present in FDB001395 successfully interacted with Tyr268 through three hydrophobic interactions. Moreover, the seven membered ring present in the molecule was also connected with Pro248 via hydrophobic contact. One of the two oxo functional groups attached to the terminal cyclic ring in FDB029219 was formed one HB interaction with Tyr273. The same terminal hexacycle ring was critically formed one hydrophobic interaction with each of Pro248 and Tyr264. Beyond that, Tyr268 was seen to connect to FDB029219 through a hydrophobic and pi-stacking. Interestingly, FDB029219 interacting with amino acids of PLpro were found to be common to interact with the co-crystal ligand, VBY. A number of HB and hydrophobic interactions were observed between FDB030757 and ligand-binding amino residues of PLpro. One of the hydroxyl groups attached to the terminal phenyl ring was potentially formed two and one HB interactions with Asp166 and Glu167, respectively. Two out of three hydroxyl groups attached to the terminal hetero-cyclic ring formed one and two HB interactions with Asn267 and Gly266, respectively. Tyr268 was seen to establish one HB interaction with an -oxo group present in between two fused rings and a terminal heterocyclic ring in FDB030757. Three important hydrophobic interactions were observed between the conserved amino acid Tyr268 and FDB030757. The hydroxyl group attached to the phenyl ring of FDB031079 was found to be very important for forming a strong HB interaction with residues Lys157 and Leu162 of SARS-CoV-2 PLpro protein. In addition, the -oxo group present in the linear chain in between two rings was connected via HB interaction with Gln269. Both the rings and the linear chain present in FDB030757 were found important for forming one hydrophobic interaction with each of amino acid residues Asp164, Tyr264, Tyr268 and Gln269 of the SARS-CoV-2 PLpro protein. It was interesting to observe that residues Asp164, Tyr264, Tyr268 and Gln269 were found to be the common interacting amino acid residues as of the standard inhibitor VBY.

3.3. Molecular dynamics simulation

The dynamic behaviour and stability of PLpro protein bound with all

potential dietary compounds as well as non-covalent inhibitor VBY were evaluated using an all-atoms 100 ns MD simulation study. Best docking poses of each food compound attached with PLpro protein were subjected to conventional MD simulations study. The MD simulation trajectories were assessed to determine different trajectories analyzing parameters such as protein backbone RMSD, root mean square fluctuation (RMSF), the radius of gyration (RoG) and Solvent accessible surface area (SASA), and binding free energy using the MM-GBSA technique. Values of each trajectory analyzing parameters in terms of maximum, minimum and average values for RMSD of both the PLpro backbone and ligand atoms, RMSF, RoG, and SASA profiles are given in Supplementary Table S1.

3.4. RMSD analyses of the SARS-CoV-2 PLpro bound with food compounds

The protein backbone RMSDs were calculated to assess the deviation of the SARS-CoV-2 PLpro protein backbone bound to all potential dietary food compounds. Fig. 4 shows the PLpro protein backbone RMSD values for each frame generated in the MD simulation study during 100 ns run with all four food compounds. It was found that PLpro protein backbone bound with proposed food compounds *viz.* FDB001395, FDB029219, and FDB031079 had consistent RMSD values with very small deviations throughout the simulation run, indicating the strong interaction stability of the SARS-CoV-2 PLpro protein-food compound complexes. Only for the dietary compound FDB030757, very little oscillation was observed in RMSD values till ~63 ns. However, such fluctuations were not consistent during the entire time span of simulation. Close observation reveals that such higher RMSD value (~4 Å) for dietary compound FDB030757 do not imply any conformational changes in protein backbone structure because the increased RMSD gradually started to maintain an equilibration state immediately after ~64 ns time span until the end of simulation run period and maintained such enough consistency without further fluctuation in the protein backbone RMSD values.

Likewise, the RMSDs of protein backbone atoms, ligand RMSDs were also calculated for all dietary compounds revealed similar RMSD profiles as three food compounds, *viz.* FDB001395, FDB029219, and FDB031079 remained consistent throughout the simulation time span. However, for another dietary compound FDB030757, a slight fluctuation was observed for a certain time period (Fig. 5). Precisely, the convergence in RMSD values for dietary compound FDB030757 was found starting from the simulation run to ~22 ns, and thereafter little fluctuation was observed for a short time period (~23–37 and ~63–100 ns) with a highest average RMSD value of 1.604 Å among all compounds, throughout the simulation period. Moreover, Fig. S2 (Supplementary data) depicts the locations of all the dietary food compounds simulated complex structures during the entire MD simulation at a 20 ns interval time period (i.e. at 20, 40, 60, 80, and 100 ns), which suggests that all proposed dietary food compounds occupied their positional conformation tightly at the active site cavity of the SARS-CoV-2 PLpro protein till the end of the simulation run, and hence probably showed almost stable conformations for the protein-ligand complexes. Largely, the low RMSD values of the SARS-CoV-2 PLpro protein backbone atoms suggest that all of the molecular systems remained stable during the entire span of MD simulation bound with selected proposed food compounds.

3.5. RMSF analyses of the SARS-CoV-2 PLpro bound with food compounds

The SARS-CoV-2 PLpro protein backbone RMSF values calculated for each residue and plotted against time of simulations is portrayed in Fig. 6. Although very high RMSF values were observed for all compounds bound with PLpro protein, however, fluctuations were not observed in a large scale. The RMSF plot indicates that all compounds attached with SARS-CoV-2 PLpro protein and each residue fluctuation have been measured within the range of 1.589–40.239 Å. Table S1 shows the maximum, lowest, and average RMSF values computed from MD simulation trajectories for each compound bound state with SARS-CoV-2 PLpro protein. It was observed that amino acid residues approximately extending from 14 to 26, 36 to 46, 181 to 196, and 219 to 234 fluctuated on higher scales for food compounds FDB029219 and FDB030757 in comparison to other compounds. These major fluctuations were observed probably due to protein structural conformations as the loop regions spanning form residues ~185–200 and 220–230, which are positioned away from the binding pocket. Moreover, these specific types of RMSF fluctuations in these amino acid residues were expected because no proposed compounds were found to be accompanied to form

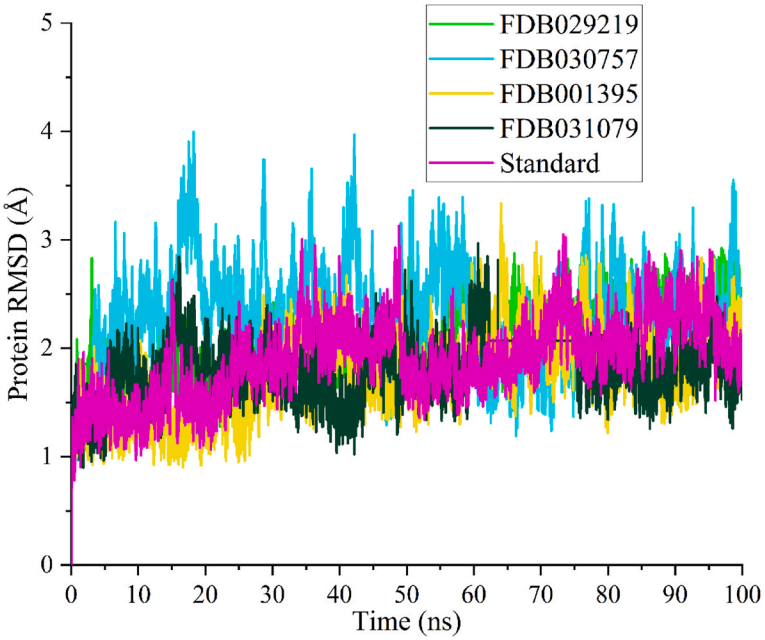

Fig. 4. RMSD values of SARS-CoV-2 PLpro protein backbone bound with proposed food compounds FDB001395, FDB029219, FDB030757, FDB031079 and non-covalent standard inhibitor (VBY).

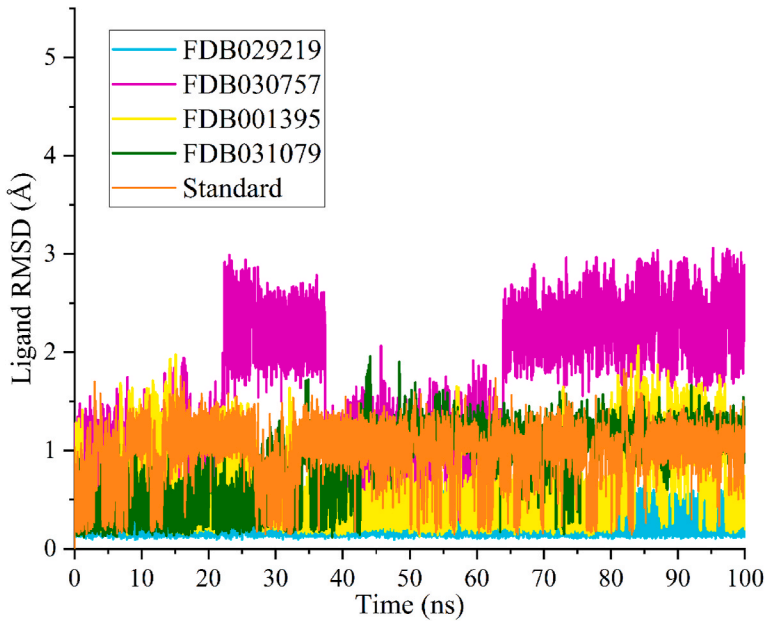

Fig. 5. Ligand RMSD bound with FDB001395, FDB029219, FDB030757, FDB031079 and standard (VBY).

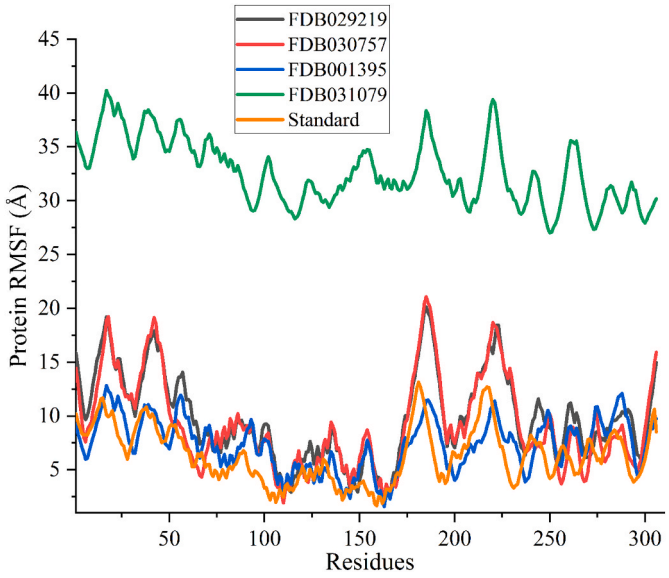

Fig. 6. RMSF values of SARS-CoV-2 PLpro backbone bound with food compounds FDB001395, FDB029219, FDB030757, FDB031079 and non-covalent standard inhibitor (VBY).

any kind of molecular binding interaction at those regions of the studied protein. Not only the present study was reveal such an interesting observation, but also similar types of fluctuations in residues level at that region of SARS-CoV-2 PLpro protein was also noted in many other studies reported earlier [62–66]. Otherwise, overall, all SARS-CoV-2 PLpro protein-ligands (i.e. complexes of FDB001395, FDB031079, and VBY) complexes disclosed a similar arrangement of RMSF values during the entire span of the simulation period. The degree of flexibility in terms of fluctuations found at the residue level at a lower scale likely indicates that there was no discernible triggering impact or local alterations associated with SARS-CoV-2 PLpro protein amino acid residues during simulation.

3.6. RoG analyses of the SARS-CoV-2 PLpro bounds with food compounds

Another important MD simulation trajectory analyzing parameter, RoG was used to assess the compound bound state of SARS-CoV-2 PLpro protein structural compactness or folding organization in a dynamic environment for all complexes, including the standard compound VBY. The average RoG values of compounds FDB001395, FDB029219, FDB030757, FDB031079 and VBY were observed as 22.633, 22.698, 22.734, 22.053, and 22.766 Å. The RoG values of each SARS-CoV-2 PLpro protein frame bound with proposed food compounds is plotted against time and displayed in Fig. 7. As presented in Fig. 7, RoG values showed that all food compounds bound to the SARS-CoV-2 PLpro protein complex remained firmly folded throughout the simulation period with no visible changes in RoG plot, except for the standard compound. In particular, the SARS-CoV-2 PLpro protein structure showed a somewhat similar pattern of RoG values bound to all proposed food compounds with a very less magnitude of fluctuations for the entire MD simulation span. However, for the non-covalent standard inhibitor VBY, little bit fluctuations were observed in RoG values indicating some changes during the protein folding state or less compactness attained for the SARS-CoV-2 PLpro protein structure with the bound state of VBY. Hence, observing such less variation in RoG values for the proposed food compounds might indicate that all compounds bound to the SARS-CoV-2 PLpro protein structure were stably folded and remained compact throughout the simulation run period. The maximum, minimum, and average values of RoG were calculated for all compounds from MD simulated trajectories and presented in Table S1.

3.7. H-bond interaction analyses of the SARS-CoV-2 PLpro bound with food compounds during MD simulation

The distribution of H-bond interactions was calculated throughout the simulation run period for all compounds, including the standard compound VBY and is displayed in Fig. 8. It was revealed that food compounds FDB001395 and FDB030757 showed maximum numbers of H-bond interaction formation during simulation in turns of creation of 4 numbers of H-bond interaction for the certain time period. The other two food compounds FDB029219 and FDB031079, also created H-bond interactions during MD simulation. However, a relatively less number of

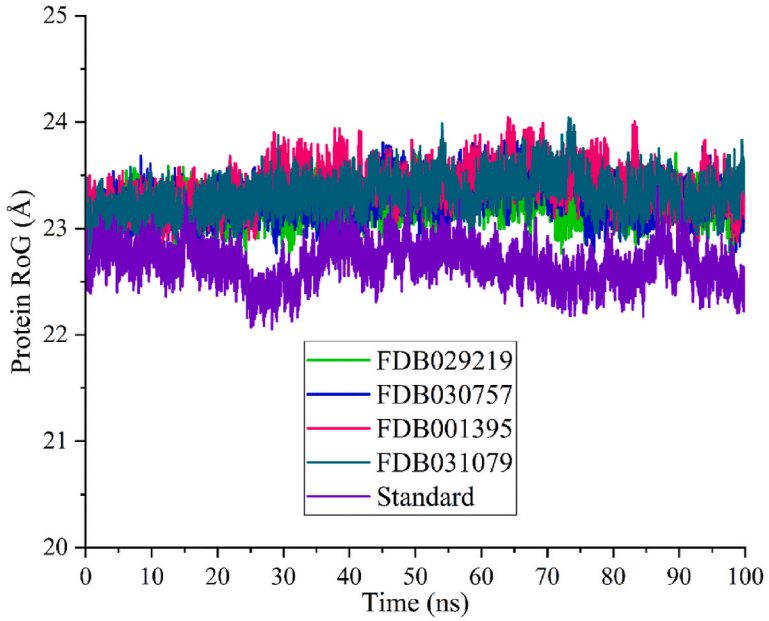

Fig. 7. RoG values of SARS-CoV-2 PLpro backbone bound with food compounds FDB001395, FDB029219, FDB030757, FDB031079 and non-covalent standard inhibitor (VBY).

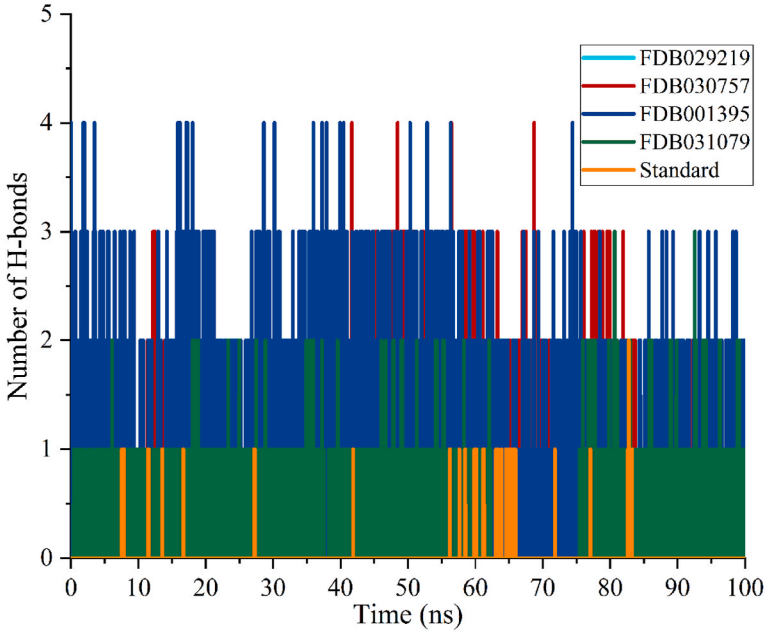

Fig. 8. Distributions of H-bond interaction of bound food compounds FDB001395, FDB029219, FDB030757, FDB031079 and standard non-covalent inhibitor (VBY) with SARS-CoV-2 PLpro protein during 100 ns MD simulation.

H-bond interactions was observed i.e. 2 and 3, respectively. On the other hand, standard inhibitor VBY created two H-bond interactions with SARS-CoV-2 PLpro protein. Interestingly, in the present study docking based inter-molecular interactions analyses also revealed similar numbers of H-bond interactions with proposed food compounds. Moreover, in large ensembles of molecular structures, H-bonding plays an essential role in interactions of molecular structures, as well as monitoring and directing structural changes and kinetic processes. Therefore, it might be postulated that, in comparision to the standard compound VBY, all proposed food compounds can tightly hold their chemical conformity inside the catalytic site of SARS-CoV-2 PLpro protein through H-bond interaction, and therefore more suitable for implicating necessary modulating or inhibitory action for the studied protein. Furthermore, to understand the actual drug binding site at the SARS-CoV-2 PLpro protein, few key amino acid residues that sustained different types of intermolecular interactions profiles with identified bioactive food compounds for a longer run period were investigated. The observed key residue interactions with each identified compound is depicted in Fig. 9. Many close-proximity residues of the catalytic triad of PLpro protein was found to be capable of successfully maintaining a biologically relevant intermolecular interactions network for the majority of the proposed compounds. In particular, residues Tyr258, Tyr262 and Gln263 were found to be critically important for establishing several types of intermolecular interaction in dynamic conditions. Such a diverse intermolecular interaction profile achieved through key residues' involvement may certainly determine a stable complex

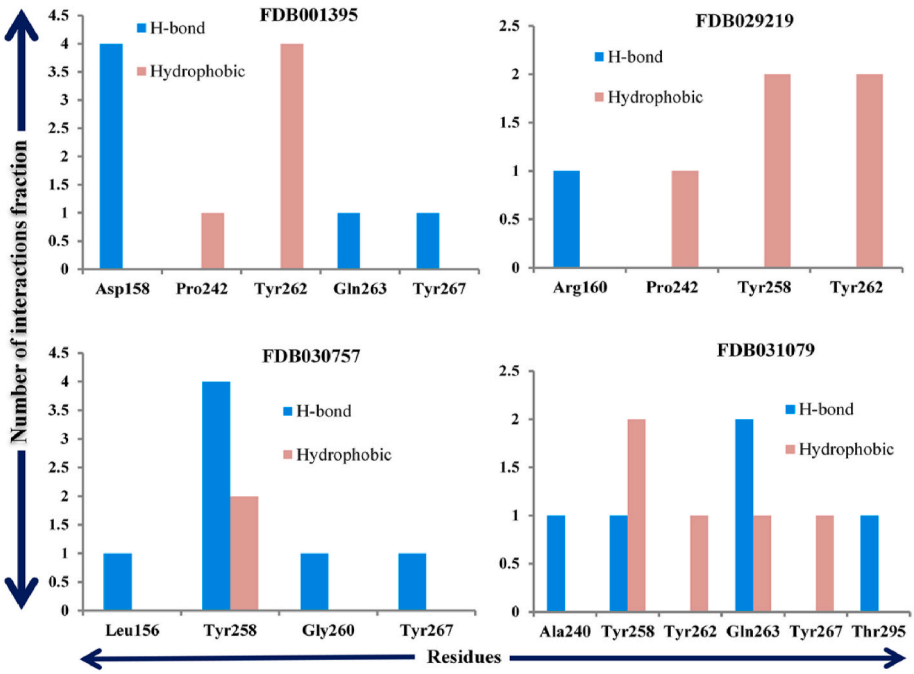

Fig. 9. Key amino acid residues of SARS-CoV-2 PLpro protein participating in different types of intermolecular interactions (H-bond and hydrophobic contacts) formation during MD simulation of the proposed dietary bioactive compounds.

structure to confirm binding poses obtained from MD simulations.

3.8. SASA analyses of the SARS-CoV-2 PLpro bound with food compounds

Fig. 10 shows the SASA traces during the MD simulation run period, which indicate that almost all compounds bound to the SARS-CoV-2 PLpro protein displayed consistent SASA values, and hence proposing smooth structural relaxation with uniform solvent density around the protein. Precisely, SASA is defined as the space of the protein that is usually exposed enough to make possible interactions with the nearest or other neighboring solvent molecules. In terms of MD simulation-based SASA analyses, changes in the accessibility of protein to solvent were calculated versus time span and found to be similar for all proposed food compounds including the standard VBY. It was found that the maximum SASA values for all compounds ranged from 14979.651 to 14655.385 Å^2. The average SASA scores for compounds FDB001395, FDB029219, FDB030757, FDB031079 and VBY were observed to be 13690.230, 13467.870, 13805.200, 13703.060 and 13715.010 Å^2, respectively. Such observation confirmed that there was no such uneven distribution of solvent accessibility of the hydrophobic core of SARS-CoV-2 PLpro protein upon binding of selected food modulator/inhibitor compounds. Moreover, the obtained consistent SASA profile for all compounds bound with SARS-CoV-2 PLpro protein alternatively also signifying folding of protein stably without any hindrances from surrounding solvent exposers and/or any specific hydrophobic interactions

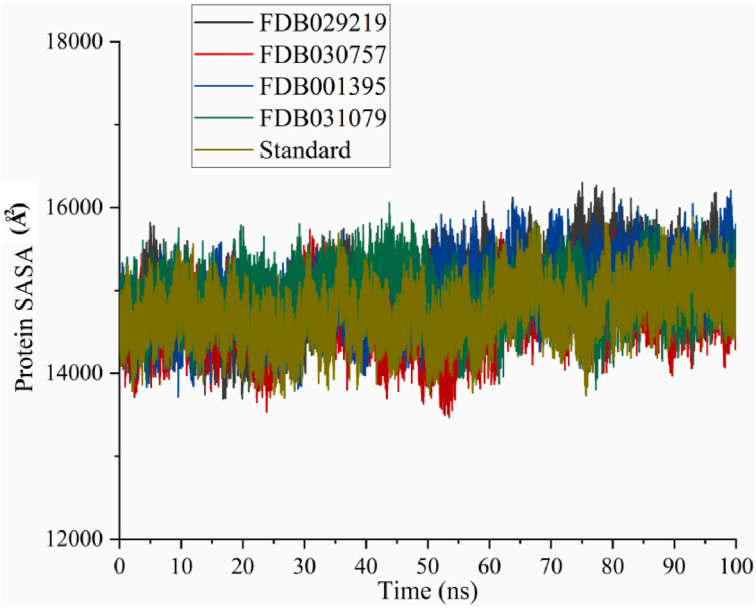

Fig. 10. PLpro backbone SASA profile bound with FDB001395, FDB029219, FDB030757, FDB031079 and standard (VBY).

that probably occurred in a dynamic state.

3.9. Importance of binding interactions of identified dietary compounds with SARS-CoV-2 PLpro protein and comparison with previously reported study outcomes

There are a number of studies that have previously reported the significance of various intermolecular interactions between SARS-CoV-2 PLpro protein and small molecular compounds identified through different experimental techniques, including *in silico* approaches like molecular docking and MD simulations. In the present study, similar and comparable forms of intermolecular interactions were also discovered at the active site region of SARS-CoV-2 PLpro protein residues and identified bioactive dietary compounds. A virtual screening study was conducted by S. Rajpoot et al. [67], reported that some naturally occurring drugs, namely Naloxone, Fluoxetine, Benzenebutyric acid, and Acetylsalicylic acid, exhibited docking based binding energy scores of −7.8, −7.5, −6.5, and −5.3 kcal/mol, respectively, against SARS-CoV-2 PLpro protein. A few amino acid residues like Pro248, Tyr264, Gly266, Tyr268, Gln269, and Tyr273 of SARS-CoV-2 PLpro were found to participate in formation of various intermolecular interactions with the reported naturally occurring drugs. In the present study, very similar residue involvement was found for most of the identified dietary compounds in the docking study. The said study also explained a 50 ns MD simulation for Naloxone and Fluoxetine which revealed conformational stability of the complexes with a lower RMSD value in dynamic conditions [67]. Earlier, screening of potential drug candidate from *Azadirachta Indica* (Neem) extracts against SARS-CoV-2 PLpro suggested that Desacetylgedunin as a potential compound exhibited a docking score of −7.3 kcal/mol. Interestingly, the study reported a relatively less stable conformational integrity for the protein-ligand complex, as large fluctuations were observed in RMSD values (~after 40 ns) studied in MD simulation. Such an observation might be due to the involvement of different amino acid residues of PLpro protein in various interaction formations [68]. Recetly, Y. Xu et al. [69], performed a high-throughput drug screening targeting SARS-CoV-2 PLpro resulting in the identification of Tanshinone IIA sulfonate sodium and chloroxine as the potential inhibitors of SARS-CoV-2 PLpro exhibiting docking based binding affinities of −8.6 and −5.9 kcal/mol, respectively. In docking study, they discovered that Tanshinone IIA sulfonate sodium interacted through π-π stacking and cation-π interaction with residues Tyr268 and Arg166, respectively. On the other hand, another compound chloroxine, establishes a binding interaction with Arg65. However, a long range MD simulation study revealed persistent associations of important amino acid residues Tyr264, Tyr273, Tyr268, and Gln269 in various interaction formations [69]. The present study also establishes a similar kind of binding interaction mechanism for the majority of the identified dietary compounds as exhibited in docking and MD simulation studies. Another study identified some structural analogues (e.g. Jun9-53-2, Jun9-72-2, and Jun9-75-4) of GRL0617 as potent inhibitor compounds for SARS-CoV-2 PLpro protein [70]. The docking study highlighted a few amino acid residues like Leu162, Asp164, Tyr268, and Gln269 as important residues involved in different types of intermolecular interactions (such as H-bond, hydrophobic, and π−π stacking) identified for studied analogue of GRL0617 [70]. In addition, for all the compounds, 100 ns MD simulation study also exhibited significantly smaller RMSD values for SARS-CoV-2 PLpro protein backbone atoms. In the present study, a very similar binding interaction profile and RMSD values were observed for all the studied dietary compounds which suggests that the proposed compounds may have better or comparable binding inhibition affinity than the standard compounds VBY or some previously reported PLpro inhibitors. In an another study by Chen et al. [71], investigated the binding interaction affinity of Ginkgolic acid as a specific potent covalent inhibitor of SARS-CoV-2 PLpro protein and highlighted a binding affinity score of −4.9 kcal/mol in docking study which was relatively lower binding affinity score than the proposed dietary bioactive food compounds. In an earlier reported study, a very small set of chemical library consisting of only 176 phytochemicals from five West African antiviral culinary herbs were screened against SARS-CoV-2 proteases. The said *in silico* study represented the pythochemical compound Vernonioside A4 as the most potent inhibitor for SARS-CoV-2 PLpro protein with a binding affinity score of −7.2 kcal/mol [72]. The docking obtained interaction analysis of Vernonioside A4 revealed that a few amino acid residues of the PLpro protein, such as Pro248, Gln250, and Try268 were found to participate in H-bond interaction. The said study also reported a 100 ns MD simulation study for the PLpro-Vernonioside A4 complex which turned out to be stable complex formation for a longer run period. The highlighted maximum RMSD value for PLpro protein backbone bound with Vernonioside A4 compound found to be ~2.5 Å. In the similar fashion, the present study was also corroborated with the outcome of the various parameters including the binding interaction profiles, conformational arrangement of the protein bound with proposed bioactive food compounds, and stability of the studied SARS-CoV-2 PLpro protein-dietary complexes, which were found to be highly consistent and may have paved the way for being responsible for modulating the biological function of the SARS-CoV-2 PLpro protein.

3.10. MM-GBSA based binding free energy estimation for protein-ligand complexes

The binding energy estimated through the MM-GBSA approach from the MD simulation trajectories is considered to be more accurate and rigorous in nature. Hence, to assess the binding affinity of the final proposed molecules, the MM-GBSA approach was considered and binding energy recorded. Total binding free energy (ΔG_{bind}) along with other components such as Electrostatic, van der Waal's energies, and calculated standard deviation values are given in Table 1. All proposed dietary molecules including the standard compound were found to have a strong binding affinity towards the SARS-CoV-2 PLpro protein. Particularly, the binding free energy of compounds FDB029219, FDB001395, FDB030757, FDB031079 and VBY was found to be −24.440, −24.914, −15.563, −28.597 and −27.263 kcal/mol, respectively. Only the binding affinity of FDB030757 was found to be bit less than other proposed food compounds and VBY, and it showed a relatively lower binding free energy score of −15.563 kcal/mol. Moreover, it was found that three of the proposed food compounds (FDB029219, FDB001395, and FDB031079) have very similar or comparable binding free energies like the standard compound VBY. This could be due to the similar chemical sub-structure found in the different proposed food compounds and similarity in the nature of binding interaction characteristics with several amino acid residues of SARS-CoV-2 PLpro protein. Particularly, numerous intermolecular interactions such as hydrogen bond, hydrophobic, electrostatics, and π-stacking interactions were formed among the various atoms of food compounds and the distinct sub-site residues of SARS-CoV-2 PLpro protein, which convey the

Table 1
Average binding free energy of FDB001395, FDB029219, FDB030757, FDB031079 and standard compound (VBY) estimated from the MD simulation trajectories.

Food compounds	Energy (kcal/mol)			
	[a]Elec.	[b]vdW	ΔG_{bind}	[c]Std. Dev.
FDB029219	−5.379	−28.266	−24.440	2.482
FDB030757	24.678	−22.002	−15.563	4.814
FDB001395	−5.938	−30.521	−24.914	2.222
FDB031079	−14.659	−34.925	−28.597	2.631
VBY	−3.166	−30.541	−27.263	4.511

[a] Electrostatic;
[b] van der Waal's;
[c] Standard deviation.

comparable binding free energies for the identified compounds. Overall, it can be illustrated that all proposed molecules possess significant binding interaction affinity towards the SARS-CoV-2 PLpro protein, as observed from the obtained binding free energy estimation from their simulated dynamic trajectories.

4. Conclusion

In the present study, to screen out potential food compounds from the FooDB database for effective inhibition or modulation of the SARS-CoV-2 PLpro protein, an exhaustive molecular docking and MD simulation was used. Following the effective implementation of several pharmacoinformatics methods, four potential SARS-CoV-2 PLpro inhibitors or modulators (as FDB001395, FDB029219, FDB030757, and FDB031079) were identified. Molecular docking revealed several significant inter-molecular binding contacts between the functional groups of the identified food compounds and the catalytic amino acids of SARS-CoV-2 PLpro protein, which were also confirmed by all-atom MD simulations studies in a dynamic state. The high binding free energy of each food compound was determined by K_{Deep} – DCNNs based application, which categorically explains the proposed compounds' better binding affinity for the SARS-CoV-2 PLpro than the standard compound VBY.

Binding interaction analysis was also compared with the existing literatures and found to be comparable binding patterns as discovered in several situations. The MD simulation study was revealed different characteristics of both the protein backbone and the food compounds such as RMSD and RMSF, RoG, SASA, H-bond interaction profile, etc., and it was discovered that the backbone of SARS-CoV-2 PLpro remained very stable even after binding with the suggested molecules in comparison to the standard inhibitor data. Using the MM-GBSA method, 10000 molecular trajectory frames from each MD simulation complex were utilized to determine the absolute binding free energy, which also demonstrated strong ΔG values for all complexes ranging from −15.563 to −28.597 kcal/mol. Overall, the extensive computational study observation explained that all proposed food compounds might be acting as crucial SARS-CoV-2 PLpro inhibitors or modulators for successful therapeutic application in COVID-19.

Availability of data and material

Not availability.

Declaration of competing interest

The authors declare that they have no known competing financial interests or personal relationships that could have appeared to influence the work reported in this paper.

Acknowledgment

This work was funded by the Deanship of Scientific Research at the Princess Nourah bint Abdulrahman University, Riyadh, Saudi Arabia, through the Research Groups Program Grant no. (RGP-1440–0021).

Appendix A. Supplementary data

Supplementary data to this article can be found online at https://doi.org/10.1016/j.jmgm.2021.108113.

References

[1] K. Steuten, H. Kim, J.C. Widen, B.M. Babin, O. Onguka, S. Lovell, et al., Challenges for targeting SARS-CoV-2 proteases as a therapeutic strategy for COVID-19, ACS Infect. Dis. (2021).
[2] G. Liu, J.H. Lee, Z.M. Parker, D. Acharya, J.J. Chiang, M. van Gent, et al., ISG15-dependent activation of the sensor MDA5 is antagonized by the SARS-CoV-2 papain-like protease to evade host innate immunity, Nat. microbiol. 6 (2021) 467–478.
[3] Z. Fu, B. Huang, J. Tang, S. Liu, M. Liu, Y. Ye, et al., The complex structure of GRL0617 and SARS-CoV-2 PLpro reveals a hot spot for antiviral drug discovery, Nat. Commun. 12 (2021) 488.
[4] D. Shin, R. Mukherjee, D. Grewe, D. Bojkova, K. Baek, A. Bhattacharya, et al., Papain-like protease regulates SARS-CoV-2 viral spread and innate immunity, Nature 587 (2020) 657–662.
[5] B.K. Maiti, Can papain-like protease inhibitors halt SARS-CoV-2 replication? ACS pharmacol. translat. sci. 3 (2020) 1017–1019.
[6] W. Rut, Z. Lv, M. Zmudzinski, S. Patchett, D. Nayak, S.J. Snipas, et al., Activity profiling and crystal structures of inhibitor-bound SARS-CoV-2 papain-like protease: a framework for anti-COVID-19 drug design, Sci. Adv. (2020) 6.
[7] D. Shin, R. Mukherjee, D. Grewe, D. Bojkova, K. Baek, A. Bhattacharya, et al., Papain-like protease regulates SARS-CoV-2 viral spread and innate immunity, Nature 587 (2020) 657–662.
[8] T. Klemm, G. Ebert, D.J. Calleja, C.C. Allison, L.W. Richardson, J.P. Bernardini, et al., Mechanism and inhibition of the papain-like protease, PLpro, of SARS-CoV-2, EMBO J. 39 (2020), e106275.
[9] H.K. Manikyam, S.K. Joshi, Whole genome analysis and targeted drug discovery using computational methods and high throughput screening tools for emerged novel coronavirus (2019-nCoV), J. pharma. drug res. 3 (2020) 341–361.
[10] V. Anirudhan, H. Lee, H. Cheng, L. Cooper, L. Rong, Targeting SARS-CoV-2 viral proteases as a therapeutic strategy to treat COVID-19, J. Med. Virol. 93 (2021) 2722–2734.
[11] Y.M. Baez-Santos, S.E. St John, A.D. Mesecar, The SARS-coronavirus papain-like protease: structure, function and inhibition by designed antiviral compounds, Antivir. Res. 115 (2015) 21–38.
[12] K. Ratia, A. Kilianski, Y.M. Baez-Santos, S.C. Baker, A. Mesecar, Structural Basis for the Ubiquitin-Linkage Specificity and deISGylating activity of SARS-CoV papain-like protease, PLoS Pathog. 10 (2014), e1004113.
[13] W. Rut, Z. Lv, M. Zmudzinski, S. Patchett, D. Nayak, S.J. Snipas, et al., Activity profiling and crystal structures of inhibitor-bound SARS-CoV-2 papain-like protease: a framework for anti–COVID-19 drug design, Sci. Adv. 6 (2020), eabd4596.
[14] J. Osipiuk, S.A. Azizi, S. Dvorkin, M. Endres, R. Jedrzejczak, K.A. Jones, et al., Structure of papain-like protease from SARS-CoV-2 and its complexes with non-covalent inhibitors, Nat. Commun. 12 (2021) 743.
[15] J.A. Henderson, N. Verma, R.C. Harris, R. Liu, J. Shen, Assessment of proton-coupled conformational dynamics of SARS and MERS coronavirus papain-like proteases: implication for designing broad-spectrum antiviral inhibitors, J. Chem. Phys. 153 (2020), 115101.
[16] M.A. Alamri, M. Tahir ul Qamar, M.U. Mirza, S.M. Alqahtani, M. Froeyen, L.-L. Chen, Discovery of human coronaviruses pan-papain-like protease inhibitors using computational approaches, J. pharm. analy. 10 (2020) 546–559.
[17] S. Dong, J. Sun, Z. Mao, L. Wang, Y.L. Lu, J. Li, A guideline for homology modeling of the proteins from newly discovered betacoronavirus, 2019 novel coronavirus (2019-nCoV), J. Med. Virol. 92 (2020) 1542–1548.
[18] S. Vardhan, S.K. Sahoo, In silico ADMET and molecular docking study on searching potential inhibitors from limonoids and triterpenoids for COVID-19, Comput. Biol. Med. 124 (2020), 103936.
[19] Y.K. Bosken, T. Cholko, Y.C. Lou, K.P. Wu, C.A. Chang, Insights into dynamics of inhibitor and ubiquitin-like protein binding in SARS-CoV-2 papain-like protease, Front. mol. biosci. 7 (2020) 174.
[20] A. Welker, C. Kersten, C. Muller, R. Madhugiri, C. Zimmer, P. Muller, et al., Structure-activity relationships of benzamides and isoindolines designed as SARS-CoV protease inhibitors effective against SARS-CoV-2, ChemMedChem 16 (2021) 340–354.
[21] L. Thurakkal, S. Singh, R. Roy, P. Kar, S. Sadhukhan, M. Porel, An in-silico study on selected organosulfur compounds as potential drugs for SARS-CoV-2 infection via binding multiple drug targets, Chem. Phys. Lett. 763 (2021), 138193.
[22] C. Mouffouk, S. Mouffouk, L. Hambaba, H. Haba, Flavonols as potential antiviral drugs targeting SARS-CoV-2 proteases (3CL(pro) and PL(pro)), spike protein, RNA-dependent RNA polymerase (RdRp) and angiotensin-converting enzyme II receptor (ACE2), Eur. J. Pharmacol. 891 (2021), 173759.
[23] P. Delre, F. Caporuscio, M. Saviano, G.F. Mangiatordi, Repurposing known drugs as covalent and non-covalent inhibitors of the SARS-CoV-2 papain-like protease, Front. Chem. 8 (2020), 594009.
[24] D. Mishra, G.S. Suri, G. Kaur, M. Tiwari, Comparative insight into the genomic landscape of SARS-CoV-2 and identification of mutations associated with the origin of infection and diversity, J. Med. Virol. 93 (2021) 2406–2419.
[25] M. Jamalan, E. Barzegari, F. Gholami-Borujeni, Structure-based screening to discover new inhibitors for papain-like proteinase of SARS-CoV-2: an in silico study, J. Proteome Res. 20 (2021) 1015–1026.
[26] B.M. Burton-Freeman, A.K. Sandhu, I. Edirisinghe, Red raspberries and their bioactive polyphenols: cardiometabolic and neuronal health links, Adva. Nutri. 7 (2016) 44–65.
[27] D. Mozaffarian, Dietary and policy priorities for cardiovascular disease, diabetes, and obesity: a comprehensive review, Circulation 133 (2016) 187–225.
[28] H. Cory, S. Passarelli, J. Szeto, M. Tamez, J. Mattei, The role of polyphenols in human health and food systems: a mini-review, Front. Nutri. 5 (2018).
[29] M. Konstantinidi, A.E. Koutelidakis, Functional foods and bioactive compounds: a review of its possible role on weight management and obesity's metabolic consequences, Medicine 6 (2019).

[30] C. Nediani, J. Ruzzolini, A. Romani, L. Calorini, Oleuropein, a bioactive compound from olea europaea L., as a potential preventive and therapeutic agent in non-communicable diseases, Antioxidants 8 (2019) 578.
[31] T.D. Natarajan, J.R. Ramasamy, K. Palanisamy, Nutraceutical potentials of synergic foods: a systematic review, J. Ethnic Foods 6 (2019) 27.
[32] T.C. Wallace, R.L. Bailey, J.B. Blumberg, B. Burton-Freeman, C.O. Chen, K. M. Crowe-White, et al., Fruits, vegetables, and health: a comprehensive narrative, umbrella review of the science and recommendations for enhanced public policy to improve intake, Crit. Rev. Food Sci. Nutr. (2019) 1–38.
[33] L. Silva, N. Pinheiro-Castro, G.M. Novaes, G.F.L. Pascoal, T.P. Ong, Bioactive food compounds, epigenetics and chronic disease prevention: focus on early-life interventions with polyphenols, Food Res. Int. 125 (2019), 108646.
[34] M.M. Ulaszewska, C.H. Weinert, A. Trimigno, R. Portmann, C. Andres Lacueva, R. Badertscher, et al., Nutrimetabolomics: an integrative action for metabolomic analyses in human nutritional studies, Mol. Nutr. Food Res. 63 (2019), 1800384.
[35] J.A. Milner, Molecular targets for bioactive food components, J. Nutr. 134 (2004), 2492S-8S.
[36] S.W. Choi, S. Friso, Epigenetics: a new bridge between nutrition and health, Adv. Nutr. 1 (2010) 8–16.
[37] T.M. Hardy, T.O. Tollefsbol, Epigenetic diet: impact on the epigenome and cancer, Epigenomics 3 (2011) 503–518.
[38] C. Tiffon, The impact of nutrition and environmental epigenetics on human health and disease, Int. J. Mol. Sci. 19 (2018).
[39] Y. Pan, Z. Deng, F. Shahidi, Natural bioactive substances for the control of food-borne viruses and contaminants in food, Food Prod., Process. Nutr. 2 (2020) 27.
[40] K.R. Bright, D.H. Gilling, Natural virucidal compounds in foods, Viruses in Foods (2016) 449–469.
[41] A. Alkhatib, Antiviral functional foods and exercise lifestyle prevention of coronavirus, Nutrients 12 (2020).
[42] M.M. Rahman, A. Mosaddik, A.K. Alam, Traditional foods with their constituent's antiviral and immune system modulating properties, Heliyon 7 (2021), e05957.
[43] W. Randazzo, M.J. Fabra, I. Falcó, A. López-Rubio, G. Sánchez, Polymers and biopolymers with antiviral activity: potential applications for improving food safety, Compr. Rev. Food Sci. Food Saf. 17 (2018) 754–768.
[44] S. Bhowmick, N.A. AlFaris, J.Z. Altamimi, Z.A. Alothman, T.S. Aldayel, S. M. Wabaidur, et al., Screening and analysis of bioactive food compounds for modulating the CDK2 protein for cell cycle arrest: multi-cheminformatics approaches for anticancer therapeutics, J. Mol. Struct. 1216 (2020), 128316.
[45] O. Trott, A.J. Olson, AutoDock Vina: improving the speed and accuracy of docking with a new scoring function, efficient optimization, and multithreading, J. Comput. Chem. 31 (2010) 455–461.
[46] W.J. Guan, Z.Y. Ni, Y. Hu, W.H. Liang, C.Q. Ou, J.X. He, et al., Clinical characteristics of coronavirus disease 2019 in China, N. Engl. J. Med. 382 (2020) 1708–1720.
[47] N.T. Nguyen, T.H. Nguyen, T.N.H. Pham, N.T. Huy, M.V. Bay, M.Q. Pham, et al., Autodock Vina adopts more accurate binding poses but Autodock4 forms better binding affinity, J. Chem. Inf. Model. 60 (2020) 204–211.
[48] P.B. Shinde, S. Bhowmick, E. Alfantoukh, P.C. Patil, S.M. Wabaidur, R.V. Chikhale, et al., De novo design based identification of potential HIV-1 integrase inhibitors: a pharmacoinformatics study, Comput. Biol. Chem. 88 (2020), 107319.
[49] S. Bhowmick, S.A. Alissa, S.M. Wabaidur, R.V. Chikhale, M.A. Islam, Structure-guided screening of chemical database to identify NS3-NS2B inhibitors for effective therapeutic application in dengue infection, J. Mol. Recogn. 33 (2020) e2838.
[50] J. Jiménez, M. Škalič, G. Martínez-Rosell, De Fabritiis, G. Kdeep, Protein–ligand absolute binding affinity prediction via 3D-convolutional neural networks, J. Chem. Inf. Model. 58 (2018) 287–296.
[51] W.L. Jorgensen, J. Chandrasekhar, J.D. Madura, R.W. Impey, M.L. Klein, Comparison of simple potential functions for simulating liquid water, J. Chem. Phys. 79 (1983) 926–935.
[52] J.A. Maier, C. Martinez, K. Kasavajhala, L. Wickstrom, K.E. Hauser, C. Simmerling, ff14SB: improving the accuracy of protein side chain and backbone parameters from ff99SB, J. Chem. Theor. Comput. 11 (2015) 3696–3713.
[53] J. Träg, D. Zahn, Improved GAFF2 parameters for fluorinated alkanes and mixed hydro- and fluorocarbons, J. Mol. Model. 25 (2019) 39.
[54] D.A. Case, T.E. Cheatham III, T. Darden, H. Gohlke, R. Luo, K.M. Merz Jr., et al., The Amber biomolecular simulation programs, J. Comput. Chem. 26 (2005) 1668–1688.
[55] S. Genheden, U. Ryde, The MM/PBSA and MM/GBSA methods to estimate ligand-binding affinities, Expet Opin. Drug Discov. 10 (2015) 449–461.
[56] J.A. Abdullah, B.J.M. Aldahham, M.A. Rabeea, F.A. Asmary, H.M. Alhajri, M. A. Islam, Synthesis, characterization and in-silico assessment of novel thiazolidinone derivatives for cyclin-dependent kinases-2 inhibitors, J. Mol. Struct. 1223 (2021), 129311.
[57] A. Onufriev, D. Bashford, D.A. Case, Exploring protein native states and large-scale conformational changes with a modified generalized born model, Proteins: Struc. Func., and Bioinform. 55 (2004) 383–394.
[58] J. Weiser, P.S. Shenkin, W.C. Still, Approximate atomic surfaces from linear combinations of pairwise overlaps (LCPO), J. Comput. Chem. 20 (1999) 217–230.
[59] D. Bajusz, A. Rácz, K. Héberger, Why is Tanimoto index an appropriate choice for fingerprint-based similarity calculations? J. Cheminf. 7 (2015) 20.
[60] N.M. O'Boyle, R.A. Sayle, Comparing structural fingerprints using a literature-based similarity benchmark, J. Cheminf. 8 (2016) 36.
[61] S. Salentin, S. Schreiber, V.J. Haupt, M.F. Adasme, M.P.L.I.P. Schroeder, Fully automated protein-ligand interaction profiler, Nucleic Acids Res. 43 (2015) W443–W447.
[62] M. Hosseini, W. Chen, D. Xiao, C. Wang, Computational molecular docking and virtual screening revealed promising SARS-CoV-2 drugs, Precis. Clinic. Med. 4 (2021) 1–16.
[63] P. Rao, R. Patel, A. Shukla, P. Parmar, R.M. Rawal, M. Saraf, et al., Identifying structural–functional analogue of GRL0617, the only well-established inhibitor for papain-like protease (PLpro) of SARS-CoV2 from the pool of fungal metabolites using docking and molecular dynamics simulation, Mol. Divers. (2021).
[64] D. Patel, M. Athar, P.C. Jha, Computational investigation of binding of chloroquinone and hydroxychloroquinone against PLPro of SARS-CoV-2, J. Biomol. Struct. Dynam. (2020) 1–11.
[65] M.A. Alamri, M. Tahir Ul Qamar, M.U. Mirza, S.M. Alqahtani, M. Froeyen, L. L. Chen, Discovery of human coronaviruses pan-papain-like protease inhibitors using computational approaches, J. pharm. analy. 10 (2020) 546–559.
[66] F. Sohraby, H. Aryapour, Unraveling the unbinding pathways of SARS-CoV-2 Papain-like proteinase known inhibitors by Supervised Molecular Dynamics simulation, PLoS One 16 (2021), e0251910.
[67] S. Rajpoot, M. Alagumuthu, M.S. Baig, Dual targeting of 3CLpro and PLpro of SARS-CoV-2: a novel structure-based design approach to treat COVID-19, Curr. Res. Structural . Bio. 3 (2021) 9–18.
[68] N. Baildya, A.A. Khan, N.N. Ghosh, T. Dutta, A.P. Chattopadhyay, Screening of potential drug from Azadirachta Indica (Neem) extracts for SARS-CoV-2: an insight from molecular docking and MD-simulation studies, J. Mol. Struct. 1227 (2021), 129390.
[69] Y. Xu, K. Chen, J. Pan, Y. Lei, D. Zhang, L. Fang, et al., Repurposing clinically approved drugs for COVID-19 treatment targeting SARS-CoV-2 papain-like protease, Int. J. Biol. Macromol. 188 (2021) 137–146.
[70] C. Ma, M.D. Sacco, Z. Xia, G. Lambrinidis, J.A. Townsend, Y. Hu, et al., Discovery of SARS-CoV-2 papain-like protease inhibitors through a combination of high-throughput screening and a FlipGFP-based reporter assay, ACS Cent. Sci. 7 (2021) 1245–1260.
[71] Z. Chen, Q. Cui, L. Cooper, P. Zhang, H. Lee, Z. Chen, et al., Ginkgolic acid and anacardic acid are specific covalent inhibitors of SARS-CoV-2 cysteine proteases, Cell Biosci. 11 (2021) 45.
[72] O.M. Ogunyemi, G.A. Gyebi, I.M. Ibrahim, C.O. Olaiya, J.O. Ocheje, M. M. Fabusiwa, et al., Dietary stigmastane-type saponins as promising dual-target directed inhibitors of SARS-CoV-2 proteases: a structure-based screening, RSC Adv. 11 (2021) 33380–33398.